HHS Public Access

Author manuscript

Stem Cells. Author manuscript; available in PMC 2016 July 01.

Published in final edited form as:

Stem Cells. 2015 July ; 33(7): 2280–2293. doi:10.1002/stem.2031.

Notch Receptor-Ligand Engagement Maintains Hematopoietic Stem Cell Quiescence and Niche Retention

Weihuan Wang[1], **Shuiliang Yu**[1], **Grant Zimmerman**[1], **Yiwei Wang**[1], **Jay Myers**[2], **Vionnie W.C. Yu**[3,4,5], **Dan Huang**[1], **Xiaoran Huang**[1], **Jeongsup Shim**[6], **Yuanshuai Huang**[7], **William Xin**[8], **Peter Qiao**[1], **Minhong Yan**[9], **Wei Xin**[1], **David T. Scadden**[3,4,5], **Pamela Stanley**[10], **John B. Lowe**[6], **Alex Y. Huang**[2], **Christian W. Siebel**[9], and **Lan Zhou**[1,*]

[1]Department of Pathology, Case Western Reserve University, Cleveland, OH 44106, USA

[2]Department of Pediatrics, Case Western Reserve University, Cleveland, OH 44106, USA

[3]Center for Regenerative Medicine, Massachusetts General Hospital, Boston, MA, USA

[4] Harvard Stem Cell Institute, Cambridge, MA, USA

[5] Department of Stem Cell and Regenerative Biology, Harvard University, Cambridge, MA, USA

[6]Department of Pathology, Genentech, Inc., South San Francisco, CA 94080, USA

[7]Department of Blood Transfusion, Affiliated Hospital of Luzhou Medical College, Luzhou, Sichuan Province, P. R. China

[8] University School, Hunting Valley, OH 44022, USA

[9] Department of Molecular Biology Oncology, Genentech, Inc., South San Francisco, CA 94080, USA

[10]Department of Cell Biology, Albert Einstein College of Medicine, New York, NY10461, USA

Abstract

Notch is long recognized as a signaling molecule important for stem cell self-renewal and fate determination. Here we reveal a novel adhesive role of Notch-ligand engagement in hematopoietic stem and progenitor cells (HSPCs). Using mice with conditional loss of *O*-fucosylglycans on Notch EGF-like repeats important for the binding of Notch ligands, we report that HSPCs with faulty ligand binding ability display enhanced cycling accompanied by increased egress from the marrow, a phenotype mainly attributed to their reduced adhesion to Notch ligand-expressing stromal cells and osteoblastic cells and their altered occupation in osteoblastic niches. Adhesion to Notch ligand-bearing osteoblastic or stromal cells inhibits wild type but not *O*-fucosylglycan-deficient HSPC cycling, independent of *RBP-J_K*-mediated canonical Notch signaling.

[*]**Correspondence:** Lan Zhou, Department of Pathology, Case Western Reserve University, Cleveland, OH 44106; lan.zhou@case.edu. Tel: (216)3681671; Fax: (216)3680494.

Author contributions

W.W., S.Y., G.Z., J.M., V.Y., X.H., D.H., Y.W., W.X., P.Q., and L.Z.: conception and design, data analysis and interpretation; P.S., D.S., J.B.L., C.S. and L.Z.: conception and design; J.S., M.Y., J.B.L., D.S., and C.S.: provision of study materials; P.S., A.H., D.S., J.B.L. and L.Z.: data analysis and interpretation, manuscript writing; L.Z.: final approval of manuscript

Disclosure of potential conflicts of interest

The authors declare no competing financial interests.

Furthermore, Notch-ligand neutralizing antibodies induce *RBP-J*$_K$-independent HSPC egress and enhanced HSPC mobilization. We therefore conclude that Notch receptor-ligand engagement controls HSPC quiescence and retention in the marrow niche that is dependent on *O*-fucosylglycans on Notch.

Keywords

HSC quiescence and niche retention; HSC egress and mobilization; Notch receptor-ligand interactions; *O*-fucosylglycans on Notch

Introduction

The hematopoietic stem cell (HSC) population is maintained throughout its lifetime by complex cell-intrinsic mechanisms and by extrinsic cues from specific bone marrow microenvironments, also called niches [1]. Osteoblasts [2, 3], endothelial cells [4-6], perivascular stromal cells [7, 8], multi-potent stromal cells (MSC) [9], and macrophages [10, 11] are components of HSC niches. Certain Notch receptors and their ligands are implicated in the regulation of specific hematopoietic progenitor subsets within distinct marrow microenvironments. For example, the Notch ligand JAG1 expressed by osteoblasts promotes expansion of HSCs [2]. In contrast, direct contact of HSCs with endothelial cells through Notch-ligand interactions promotes HSC proliferation and prevents HSC exhaustion [5]. Although Notch family members were first identified as cell adhesion molecules by cell aggregation assays in *Drosophila* studies [12, 13], the precise role and the physiological significance of Notch receptors as adhesion molecules in HSCs has not been defined in HSCs.

We previously generated a pan-Notch loss-of-ligand-binding mouse model by targeting *Pofut1*, the gene that encodes POFUT1, the enzyme that transfers *O*-linked fucose to conserved serine or threonine residues of Notch extracellular EGF-like repeats [14-16]. *O*-fucose modification of Notch is essential for both Notch-ligand interactions and Notch signaling activation [17-20]. Using conditional *Pofut1*-deficient (*Mx1-Cre/Pofut1*$^{F/F}$) mice, we found that deletion of *Pofut1* causes a myeloproliferative disorder [21]. The cell-autonomous dysregulation of myeloid hyperplasia is largely accounted for by loss of binding of *Pofut1*-deficient HSCs to Notch ligands.

Here we further examine the effect of conditional *Pofut1*-deletion on HSPC homeostasis, quiescence and HSPC interactions with the marrow microenvironment. Our studies reveal that *Pofut1*-deficient HSPCs are less adhesive to Notch ligand-expressing marrow stromal or osteoblastic cells, display a more active cycling activity and a more dispersed endosteal niche distribution, and are increased in number in the peripheral circulation and exhibit higher sensitivity to mobilizing stimuli. In line with these findings, we observe that mice receiving neutralizing antibodies to Notch ligands DLL4 or JAG1 exhibit increased steady-state HSPC egress and increased HSPC mobilization. These observations reveal that *O*-fucose-modified Notch receptors expressed by HSPCs are important for engaging Notch ligands expressed by niche cells, and indicate that these interactions facilitate HSPC niche retention and the maintenance of quiescence.

Materials and Methods

Mice

The Institutional Animal Care and Use Committee approved all aspects of the animal research described in this study. *Mx1-Cre/Pofut1*$^{F/F}$ and Col2.3-GFP mice were maintained as described [19, 21].

Bone marrow cell isolation, FACS, cell sorting, transplantation, and quantitative RT-PCR

Marrow mononuclear cells were lineage depleted with biotin-conjugated rat anti-mouse antibody cocktails followed by goat anti-rat IgG magnetic beads (Miltenyi), stained with streptavidin-APC-Cy7, FITC-anti-CD34, APC-anti-c-kit, PE-Cy7–anti–Sca-1, PE-anti–Flk2/Flt3, and sorted using FACSAria (BD Biosciences). Lineage depleted cells were further enriched for c-Kit^{+} cells using CD117 microbeads (Miltenyi). Cell surface marker analysis, bone marrow transplantation and qRT-PCR were performed as described [22].

Cell cycle analysis and Ki67 staining

Cell cycle analysis was performed after incubation with Hoechst 33342 and Pyronin Y followed by labeling with FITC-anti-lineage antibodies, APC-anti-c-kit and PE-Cy7-anti-Sca-1 [23]. BrdU labeling was determined as described [24]. For Ki67 staining, lineage-depleted cells were first stained with streptavidin-APC-Cy7, APC-anti-c-kit, PE-Cy7-anti-Sca-1, and treated with Cytofix/Cytoperm reagents according to the manufacturer's instructions (BD Biosciences). Cells were incubated with PE-anti-Ki67 antibody and propidium iodide (PI) in BD Perm/Wash buffer and analyzed using FACS.

Notch ligand neutralization

Humanized IgG1 neutralizing monoclonal antibody specific for the DLL4 extracellular domain (ECD) was described previously [25]. Neutralizing monoclonal antibody specific for the JAG1 ECD and the corresponding isotype control antibodies were generated and tested in a similar fashion. Antibodies were injected i.p. at 15 mg/kg body weight twice weekly, 3-4 days apart, for a total of 4 doses.

HSPC mobilization

HSPC mobilization assays were performed as described [26]. Briefly, mice were injected subcutaneously with 2.5 μg G-CSF, twice daily for 2 days, followed by subcutaneous injection of 5mg/kg AMD3100 (Sigma). Blood (250 μl) and hematopoietic tissues were collected 1h later for determination of circulating, splenic and marrow HSPC frequencies.

HSPC adherence, and chemotaxis assays

For osteoblast adherence assay, primary osteoblasts were isolated from calvaria dissected from 2-5-day-old Col2.3-GFP mice using modified methods as described [27]. Each calvarium was placed in digestion media (α-MEM containing 0.04% Trypsin and 0.01 mg/ml collagenase P) for 20 min at 37°C in a 6-well plate, and shaken vigorously for 20 sec every 5 min. Released cells were discarded. Additional digestion buffer was added to minced calvarium with double the amount of collegenase P (Roche) and incubated for 60

min with shaking every 5 min. Calvarium was incubated at 37°C overnight with the addition of 3.75 ml of culture medium (α-MEM containing antibiotics and 15% FBS), followed by vigorous pipetting. Dissociated cells were collected after centrifugation and allowed to attach to the plate for 4-6 h followed by washing with PBS. Cells were cultured in culture medium for 3 days, trypsinized and replated at 10,000-15,000 cells/cm^2, and the medium was changed every other day. For the modified HSPC adherence assay, confluent OP9 cells, or primary osteoblasts (2×10^4) were seeded in a 48-well plate. LK cells (1.5×10^5) suspended in 200 μl RPMI, supplemented with 10% FBS, were seeded into each well and incubated for 1 hour at 37°C. After controlled agitation on a plate mixer (Gyrotory shaker G2, 120 rpm) for 30 sec, non-adherent cells were removed by pipetting and a gentle wash of the co-culture plate and counted using a hemacytometer. Ratios of adherent LK cells to those initially added were calculated. To determine the extent to which adhesion was dependent on Notch receptor-ligand interactions, LK cells were seeded with control Ret10 cells or osteoblastic cells in the presence of recombinant DLL1-Fc (30 μg/ml) (AdipoGen) or human IgG Fc for 1 h at 37°C, followed by controlled agitation and enumeration of non-adherent cells as described above. To determine the efficacy of ligand neutralizing antibodies to block HSPC adhesion, primary calvarium osteoblasts were pre-incubated with antibodies at either 0.1 mg/ml or at 0.4 mg/ml for 30 minutes before the addition of LK cells. For chemotaxis assay, dual-chamber chemotaxis assays were performed using 24-well plates with 5 μm pore size inserts (Costar/Corning) [28]. SDF-1-containing (0, 10 ng/ml or 100 ng/ml) (R&D Systems) medium was added to the lower chamber, and 200 μl of LK cells in suspension (1×10^6/ml) were placed in the upper chamber. Cells migrated to the lower chamber were counted following 2 hour incubation.

Notch1 and Notch2 recombinant protein binding assays

Chimeric proteins Notch1 and Notch2 EGF1-15 (N1/2 1-15EGF) fused with human IgG Fc were prepared from FX-deficient CHO cells either in the absence or presence of fucose as described [29]. Binding assays were performed by incubating OP9 cells with chimeric proteins in PBS with Ca^{2+} and Mg^{2+} for 30 min at room temperature, and analyzed by FACS using PE-anti-IgG Fc (Sigma) [21].

SDF-1/CXCL12 ELISA

Bone marrow extracellular fluid was obtained by flushing each femur and tibia with 1000 μL HBSS, and the supernatant was harvested after centrifugation at 400*g* for 5 minutes. CXCL12 protein quantification in bone marrow extracellular fluid was determined by ELISA (Mouse CXCL12/SDF-1 alpha Quantikine ELISA Kit; R&D System) according to the manufacturer's instructions.

Multi-photon intravital imaging

Intravital 2-photon imaging preparation, data acquisition and data analysis were performed as previously described [24, 30]. Briefly, $Lineage^-c\text{-}kit^+Sca\text{-}1^+$ (LSK) cells ($5\text{-}15\times10^4$) were injected into the tail vein of lethally-irradiated recipient mice. At indicated times after i.v. transfer, mice were anaesthetized and a small incision was made in the scalp so as to expose the underlying dorsal skull surface. For femur bone marrow imaging, donor cell homing to

the marrow of shaved femur was imaged using a SP5/AOBS/2-photon microscope tuned to 860 nm (Leica Microsystems & Coherent Inc., Lawernceville, GA) while mice were under inhaled anesthesia (1-2% isoflurane) on a warmed microscope stage (37°C). To highlight the bone marrow vasculature, 25-60 μl TRITCBDextran (10 mg/ml) (2000 Kd; Life Technologies) was injected into recipient mice 5 min prior to the imaging experiments. Simultaneous visualization of bone endosteum, vasculature, osteoblastic cells, and HSC was achieved by second harmonic generation (SHG) microscopy, Dextran dye, GFP signals, and cells with SNARF signals, respectively. Fluorescent images from optical sections of individual *xy*-planes were collected through pre-determined, fixed optical *z*-slices. This data set was then analyzed using imaging software (Imaris; BitPlane, Inc., Saint Paul, MN), which allows simultaneous tracking of object positions in 3 dimensions over time with statistical analysis.

Immunohistochemistry staining

Femurs were fixed in 4% paraformaldehyde overnight at 4°C, and then decalcified for 24 hours in decalcifying solution (Thermo Scientific). After rehydrated in 30% sucrose solution for 48 hours, tissues were snap-frozen in OCT (TissueTek). Whole longitudinal femur were cut into 7μm sections using a cryostat, and fixed with 4% paraformaldehyde for 10 minutes. Slices were washed with PBS and blocked in blocking solution (0.2% Triton containing 3% BSA in PBS) for 1 hour at room temperature. Sections were stained with rat anti-VEGFR3 (BD Biosciences) at a dilution of 1:50 overnight at 4°C, washed in PBS and stained with anti-rat secondary antibody (Vector laboratories) for 1 hour at room temperature, followed by PBS washing and treatment with Horseradish Peroxidase (HRP; Vector laboratories) for 30 minutes at room temperature. 3,3'-diaminobenzidin served as the HRP chromogenic substrate. The sections were then counterstained with hematoxylin, and microscopic images were captured digitally. The numbers of VEGFR3+ vessels were enumerated on 10 random fields under 200X magnification.

Statistical analysis

Data are presented as means ±SD, unless otherwise stated. Statistical significance was assessed by Student *t* test.

Results

Pofut1-deficiency leads to transient decreases in marrow HSPCs but increases in HSPC cycling and proliferation

We previously observed that after *Pofut1* deletion in *Mx1-Cre/Pofut1*$^{F/F}$ mice, myeloproliferation is induced through both cell-intrinsic and stromal environment-dependent mechanisms, and displays a progressive increase in severity with time [21]. We report here our examination of cell-intrinsic changes of HSCs and progenitors in relation to their ability to bind Notch ligands at earlier stages after *Pofut1* deletion. Four weeks after the last dose of pIpC injection, the total LSK ($Lin^{-}Sca\text{-}1^{+}c\text{-}kit^{+}$) number is decreased by ~39% in *Mx1-Cre/Pofut1*$^{F/F}$ mice when compared to control mice (Fig 1A). All HSPC subpopulations as well as common lymphoid progenitor (CLP) cells are proportionally decreased (Fig 1B). At 4-5 months following *Pofut1* deletion, long-term HSCs (LT-HSC)

and CLPs remain suppressed, while the other subpopulations appear to recover to control numbers (Fig 1C). BrdU labeling reveals an increased proliferation of *Pofut1*-deficient progenitor cells (Fig 1D). Furthermore, *Pofut1* deletion results in a decreased number of LSK cells in G_0 and increased cells in G_1 phase (Fig 1E). These changes in cell cycling are cell-intrinsic as they persist in WT recipients receiving *Pofut1*-deficient LSK cells (Fig 1F). By qRT-PCR analysis, we find that these cycling changes are accompanied by down-regulation of *p21* and *EGR1* and increased expression of *cyclin-D1* and *cdk4* in *Pofut1*-deficient HSPCs (Fig 1G) [23, 31, 32], suggesting reduced expression of *p21* and deregulation of *cyclin-D1* and *cdk4* as likely molecular mechanisms underlying the enhanced proliferative activity of *Pofut1*-deficient HSPCs.

Pofut1-deficiency leads to increased HSPC circulation and mobilization without affecting HSPC chemotaxis or expression of CXCR4 and integrins

The paradoxical findings of reduced marrow HSPCs associated with enhanced cell cycling and proliferation, led us to suspect that there is increased HSPC exit from the marrow in *Mx1-Cre/Pofut1*$^{F/F}$ mice early after *Pofut1* deletion. Indeed, we find that circulating LSK and LK ($Lin^{-}c\text{-}kit^{+}$) cells in the periphery are increased 3.7- and 3.3-fold, respectively, in *Mx1-Cre/Pofit1*$^{F/F}$ mice compared to controls (Fig 2A-B), and their total white cell counts are also modestly increased (Fig 2C). LSK and LK cells also accumulate in the spleen of *Mx1-Cre/Pofut1*$^{F/F}$ mice, increasing ~7.4- and 2.9-fold, respectively, compared to control mice (Fig 2D-E), consistent with increased colony forming units in the CFU-C assay (Fig 2F). The frequencies of HSPCs are also increased in the periphery and in the spleen in lethally-irradiated wild type mice receiving *Pofut1*-deleted marrow cells (Fig S1). Furthermore, after G-CSF and AMD3100 treatment [26], *Mx1-Cre/Pofut1*$^{F/F}$ mice have 5.6- and 11- fold more LSKs and LKs in the periphery (Fig2 G-H) compared to non-mobilized *Mx1-Cre/Pofut1*$^{F/F}$ mice (Fig2 A-B). These mice also display a 2- and 2.5-fold increase in LSK and LK mobilization to the periphery and a 5-fold increase in LSK accumulation in the spleen compared to similarly treated control mice (Fig 2G-I). There is no significant increase of LK cells mobilized to the spleen in *Mx1-Cre/Pofut1*$^{F/F}$ mice compared to similarly treated control mice (Fig 2J). These findings imply that *Pofut1*-deficient HSPCs exit from the marrow in a more rapid and a cell-autonomous manner, and are more responsive to mobilizing stimuli.

In comparison, chemotaxis of *Pofut1*-deficient HSPCs to SDF-1 is not different from controls (Fig S2A). Expression of CXCR4 and key adhesion molecules including α_4 (CD49d), α_5 (CD49e), β_1 (CD29) or β_2 integrins (CD18), and CD44 (Fig S2B), as well as membrane-bound activated β_1 integrin (recognized by 9EG7 clone) (Fig S2C), is largely unchanged, relative to control cells. Transcripts of the chemotactic chemokine SDF-1 in stromal cells of *Mx1-Cre/Pofut1*$^{F/F}$ mice are surprisingly increased (Fig S2D), whereas SDF-1 protein level in marrow extracellular fluid is not changed (Fig S2E). These findings imply that *Pofut1*-deficient HSPCs exhibit an enhanced marrow egress phenotype that is largely independent of integrin-mediated adhesion or CXCR4/SDF-1 signaling.

Pofut1-deficient HSPCs have decreased adhesion to Notch ligand-expressing osteoblasts and stromal cells and are insensitive to cycling suppression mediated by Notch-ligand engagement

Next, we sought to understand the molecular mechanisms underlying the decreased retention of *Pofut1*-deficient HSPCs in the marrow. We asked whether Notch receptor-ligand engagement contributes to bone marrow localization of HSPCs and promotes their quiescence. To test this, we first examined the ability of Notch1 and Notch2 extracellular domains (ECDs) to bind to Notch ligands as a function of *O*-fucosylation. Fusion proteins comprising EGF1-15 of Notch1 or Notch2 ECD and IgG Fc were generated either as non-fucosylated forms (N1/N2 1-15EGF) or as fucosylated forms (N1/N2 1-15EGF+fucose) [29]. These peptides contain EGF12, one of the EGF repeats critical for Notch binding to canonical Notch ligands [33, 34]. The binding assessment reveals that both fucose-modified N1 and N2 peptides (N1/N2 1-15EGF+fucose) bind minimally to OP9 parental cells (data not shown) but bind more efficiently to OP9-DLL1 (Fig S3), OP9-JAG1 and OP9-DLL4 at all concentrations tested, relative to the non-fucose modified peptides (N1/N2 1-15EGF) (Fig 3A-B). We then asked whether *O*-fucose deficiency also modulates marrow LSK interactions with Notch ligand-expressing stromal cells. We observe that *Pofut1*-deficient and control progenitors display a similar basal level of adhesion to OP9 cells, a process mediated mostly by integrins, selectins, and immunoglobulin gene superfamily members [35]. We observe that the proportion of adherent cells further increase by 15.4%, 25%, and 23%, when WT progenitors were cultured with OP9 cells expressing JAG1, DLL1, or DLL4, respectively (Fig 3C). This Notch ligand-dependent enhanced adhesion to OP9-DLL1 cells is completely blocked by the addition of recombinant DLL1 (Fig 3E). By contrast, *Pofut1*-deficient progenitors (Fig 3C) or CD150-expressing stem cells (Fig 3D) do not display any increase in adhesion to Notch ligand-expressing OP9 cells. When primary calvarium osteoblastic cells derived from Col2.3-GFP mice, which express JAG1 and DLL1 but minimal DLL4 (Fig S4), were used in co-culture, we observe that the proportion of adhesive cells is 39.9% for WT and 26.9% for *Pofut1*-deficient cells, respectively (Fig 3F; $p<0.05$). Furthermore, co-culture with Notch ligand-expressing OP9 cells decreases the fraction of WT LSKs in G_1 and S/G_2 (from 82% for control Ret10, to 63% and 51% for OP9-DLL1 and OP9-DLL4, respectively), and concomitantly increases the fraction of cells in G_0 phase (from 17% for Ret10 to 37% and 48% for OP9-DLL1 and OP9-DLL4, respectively). However, the cycling of *Pofut1*-deficient LSK cells is minimally affected by co-culture with Notch ligands (Fig 3G). To confirm that loss of adhesion is caused by loss of *O*-fucose on Notch and is not due to reduced Notch signaling, we tested the adherence of progenitors in *Mx1-Cre/RBP-*$J_K^{F/F}$ mice, a different genetic model of global Notch signaling inactivation. We observe that HSPCs deficient in global Notch signaling due to loss of the RBP-J_K co-repressor maintain a level of adhesion to Notch ligand-bearing OP9 cells that is similar to the level of adhesion observed with WT cells, and find that adhesion is similarly blocked by recombinant DLL1 (Fig 3H). Similar to control cells exposed to DLL1, *RBP-*J_K-deficient progenitors respond with an increase in the fraction of cells in G_0 phase (from 10% to 29% compared to from 17% to 27% for controls), and a reduction in the fraction of cells in G_1 and S/G_2 (from 90% to 70% compared to 82% to 73% for controls) (Fig 3I). Together, these data support the conclusion that adhesion between HSPCs and osteoblasts or stromal cells occurs through Notch receptor-ligand coupling, which in turn

suppresses cell cycling and maintains cell quiescence, and these processes are largely independent of *RBP-J_K*-mediated Notch signaling.

Loss of Notch *O*-fucosylation leads to aberrant HSC endosteal niche occupancy

We then sought to determine whether disrupted coupling of *O*-fucose-deficient HSPCs with their marrow supporting cells, *in vivo*, in turn alters HSPC niche locations (Fig 4A). Using 2-photon microscopy, we observe a striking dispersion of *Pofut1*-deficient LSK cells in the bone marrow relative to the endosteum when compared to control LSKs (Fig 4B). While 91% of control cells are found within 20 μm of the endosteum, with an average distance of 12 μm to the endosteum, only 49% of *Pofut1*-deficient cells are within the same distance range, with an average distance of 28.7 μm to the endosteum (Fig 4C-D; $p<0.01$). We further analyzed the relative spatial relationship between HSPCs and bone-lining osteoblastic cells in mice expressing GFP^+ osteoblastic cells. On average, *Pofut1*-deficient LSKs are positioned further away from osteoblastic cells than controls (16.9 μm for *Pofut1*-deficient LSKs and 9.6 μm for control LSKs). While 96% of the control cells are within 20 μm of a GFP^+ osteoblast, only 68% of *Pofut1*-deficient cells are localized within that range ($p<0.01$). We also found that many cells closer to the GFP^+ osteoblasts are also in the immediate proximity to blood vessels, but there are no obvious differences in the relative distribution around blood vessels between *Pofut1*-deficient and control LSKs (data not shown). We did not determine whether the vessels were arteriolar or sinusoidal [36].

Blocking Notch ligands JAG1 and DLL4 enhances HSPC circulation and mobilization, largely independent of *RBP-J_K*- activated Notch signaling

It was important to examine whether enhanced *Pofut1*-deficient HSPC egress was caused by the loss of Notch receptor-ligand binding or by defective ligand-induced Notch signaling. We first inhibited Notch receptor-ligand binding by administering neutralizing humanized monoclonal antibodies targeting mouse Notch ligands DLL4 or JAG1, and then asked if this changed HSC homeostasis and distribution. anti-JAG1 was chosen because JAG1 is expressed in bone marrow stromal cells, endothelial cells, and murine osteoblasts [2, 37, 38]. anti-DLL4 was chosen because DLL4 is also expressed by endothelial cells [5] and osteolineage cells (Yu et al., manuscript accepted to J Exp Med). When tested *in vitro* using the primary calvarium osteoblasts, both anti-JAG1 and anti-DLL4 decrease the adhesion of marrow progenitor cells with the primary calvarium osteoblasts. anti-JAG1 shows a stronger suppression of adhesion than DLL4-blocking antibody (Fig S5), consistent with JAG1 being expressed at higher level than DLL4 in the calvarium osteoblasts (Fig S4). In mice receiving these antibodies, we found that circulating LSKs in the peripheral blood increase from 94 cells/ml in mice receiving isotype control antibody to 237 cells/ml ($p<0.05$) and 311 cells/ml ($p<0.01$) in mice receiving anti-JAG1 or anti-DLL4, respectively (Fig 5A-B). The frequencies of circulating LK cells also increase (Fig 5C). This enhanced circulation appear to be most significant for HSPCs, as white cells increase only to a very modest extent (Fig 5D) while platelet numbers (data not shown) do not change significantly. We observe an increase in circulating granulocytes and a decrease in circulating T lymphocytes in mice receiving anti-DLL4 but not in mice receiving anti-JAG1 (Fig 5E). Furthermore, splenic LSK and LK cells both increase after JAG1 and DLL4 antibody blockade, while marrow HSPCs show a trend of increasing after DLL4 but not after JAG1 blockade (Fig 5F-I). We

also observe an increase in marrow HSPC proliferation following DLL4 but not after JAG1 blockade (Fig 5J). DLL4 blockade leads to variable hepatic sinusoidal dilation (Fig S6A), as also reported by others [39], and an increase of $VEGFR3^+$ sinusoidal endothelial cells in the marrow (Fig S6-BC) [40]. JAG1 blockade does not alter hepatic sinusoidal or $VEGFR3^+$ sinusoidal endothelial cells in the marrow. Both DLL4 and JAG1 blockade modestly increase the expression of SDF-1/CXCL12 transcripts in stromal cells (Fig S6D) but mildly decreases SDF-1 protein expression in bone marrow plasma (Fig S6E).

In mice receiving JAG1- or DLL4-blocking antibody, the HSPC mobilizing agents G-CSF and AMD3100 induce the accumulation of 13.6- and 10.3-fold more LSKs and 5.6- and 6.8-fold more LKs in the periphery, respectively (Fig6 A-B), relative to non-mobilized mice (Fig5 B-C). This represents a 58% increase in circulating LSK cells in mice receiving the mobilizing agents and DLL1 or JAG1 blockade, relative to mice receiving the mobilizing reagents and the control antibody (2031/ml for control mice, 3201/ml with JAG1 blockade and 3208/ml for DLL4 blockade; $p<0.05$) (Fig 6A). We did not observe significant changes in either peripheral white cell counts or frequencies of granulocytes and lymphocytes in mice receiving blocking antibodies, relative to control mice (Fig 6C-D). The frequencies of splenic and marrow HSPCs as well as HSPC proliferation indexes also remain largely unaltered (Fig 6E-G). These observations imply that proliferative and mobilizing signals generated by G-CSF and AMD3100 exceed those signals consequent to Notch ligand blockade, and indicate that HSPC exit is further enhanced when ligand antagonism is followed by application of the mobilizing agents.

Next, to determine if the observed HSPC mobilizing effect of Notch ligand blockade is due to reduced Notch ligand-induced signaling, we tested HSPC mobilization and distribution in *Mx1-Cre/RBP-*$J_K^{F/F}$ mice. Overall, mice deleted in *RBP-*J_K (Fig S7) as well as the control mice (*Mx1-Cre/RBP-*$J_k^{F/+}$ or *RBP-*$J_k^{F/F}$, all treated with pIpC) display a slight increase in marrow HSPC frequency (Fig 7A) due to modest myeloproliferation in these mice at the time when the study was performed (4-5 weeks after *RBP-*J_K deletion) (Fig 7B). Modest increases in steady state circulating HSPCs and spleen-residing LSK cells are also observed in mutant mice, relative to control mice (Fig 7C-E). Although mobilizing reagents could further induce mobilization, there is no significant increase in mobilized HSPCs in *RBP-*J_k-deficient mice relative to similarly treated control mice (data not shown). Further, after receiving ligand blocking antibodies, *Mx1-Cre/RBP-*$J_k^{F/F}$ mice exhibit a milder but still significant increase in HSPC egress when compared to similarly treated control mice (Fig 7F-J) or wild type mice (Fig 5). Marrow HSPC frequencies are not altered after DLL4 or JAG1 blockade (Fig 7K-L). Compared to JAG1 blockade, DLL4 blockade induces a stronger egress of HSPCs (Fig 7F-G and Fig 7I-J) and a 2.4-fold increase of peripheral white cell numbers (Fig 7H). Therefore, although mice deficient in *RBP-*J_k-dependent canonical Notch activity exhibit a modest increase of HSPC exit in steady state, they are still capable of responding to Notch ligand blockade. These findings imply that the increased egress and the sensitivity to mobilizing signals of *Pofut1*-deficient HSPCs are primarily caused by the disengagement of Notch-ligand binding, and secondarily by loss of *RBP-*J_K-dependent Notch transcriptional activation.

Discussion

Using a mouse model in which HSPCs are defective in Notch receptor-ligand binding due to the conditional absence of *Pofut1*, we observe a transient reduction of HSPCs in the marrow in association with an increase in circulating HSPCs and their accumulation in the spleen. Unlike wild type HSPCs that display suppressed cell cycling upon adhering to Notch ligand-expressing stromal or osteoblastic cells, HSPCs expressing non-fucosylated Notch exhibit a decreased adherence to these supporting cells, display greater cell cycling, and also exhibit a more dispersed distribution relative to osteoblastic endosteal-lining cells. Consistent with these findings, Notch ligand blockade results in a similarly enhanced HSPC exit from the marrow. In summary, these findings support a novel role of Notch in HSPCs as an adhesion molecule that contributes to HSPC retention within the endosteal niche. These studies reveal that functional Notch-ligand engagement is dependent on the *O*-fucosylation of Notch, and hence a loss of *O*-fucosyl modification of Notch, or disruption of Notch receptor-ligand binding by antibodies, results in increased HSPC egress and HSPC mobilization.

Supporting cells in marrow niches interact with HSPCs and support HSPC function through a complex network of adhesion molecules and external regulators, including cytokines and chemokines [2, 3, 7, 41-44]. Although Notch functions as an adhesion molecule for mast cells [45, 46], evidence supporting a role for Notch receptor-ligand pairing in HSPC function has largely come from *in vitro* studies and a transgenic mouse model in which elevated levels of JAG1-expressing osteoblastic cells increase bone marrow numbers of HSPCs [2]. Recently, Guexguez et al report that human HSCs are enriched in the endosteal osteoblastic niche close to the osteoprogenitors and vasculature. The ability of interacting with JAG1 is a signature of human HSC and supports HSC regenerative potential [47]. Here we provide new evidence for a role of Notch in HSPC regulation. Firstly, we observe that a fragment of Notch ECD interact efficiently with OP9 cells expressing Notch ligand only when soluble Notch ECD is modified by *O*-fucose. Secondly, HSPCs display stronger adhesion to Notch ligand-expressing compared to control stromal cells, and this form of adhesion could be completely inhibited by recombinant ligand proteins. Thirdly, we show that adhesion of HSPCs to osteoblasts and stromal cells is completely abolished in *Pofut1*-deficient HSPCs due to the loss of the *O*-fucosylglycans on Notch EGF-like repeats that are important for the binding of Notch ligands. Finally, blocking Notch ligand JAG1 or DLL4 elicit a similar phenotype to that observed in *Pofut1*-deficient mice. Combined with our observations of altered HSPC cell cycling and endosteal localization associated with the loss of *Pofut1*, and the enhanced egress of *Pofut1*-deficient HSPCs, these observations lead us to conclude that Notch functions as an adhesion molecule to support HSPC retention, quiescence and homeostasis.

Although both *Pofut1* deficiency and Notch ligand antagonism elicit an increase in steady state HSPC emigration, distinct mechanisms may be responsible for each condition. In the case of *Pofut1*-deficiency, increased HSPC exit is accompanied by an increase in HSPC cell cycling, HSPC hyperproliferation, and increased signaling in response to cytokines (Wang et al, manuscript in preparation). These findings, in association with the dispersed location of *Pofut1*-deficient HSPCs in the endosteal niche, suggest that both displacement of weakly retained HSPCs, as well as expansion of proliferating HSPCs, could be responsible for the

increase in circulating HSPCs and their pronounced accumulation in extramedullary organs. A similar mechanism is likely to play a role in the setting of DLL4 antagonism but is not a likely explanation of the consequences of JAG1 blockade, as only DLL4 but not JAG1 blockade is associated with an increase of the HSPC proliferation index and the expansion of both marrow and splenic LSK cells. This could be explained by the increase in VEGFR3-expressing sinusoidal endothelial cells found in the marrow following DLL4 blockade, and hence an expansion of the proliferative endothelial niche in the marrow, consistent with the reported role of DLL4 in the suppression of endothelial sprouting [48]. Alternatively, a stronger mobilizing effect associated with DLL4 antibody could be accounted for by either less efficient access of JAG1 antibody to its targets in the marrow, despite that JAG1 antibody could efficiently block the adhesion of progenitors with the calvarium osteoblasts *in vitro*, or by the mobilization of cells associated with the endothelium and sinusoids after DLL4 blockade. Enhanced HSPC mobilization following either JAG1 or DLL4 blockade could also be contributed by a modest down-regulation of SDF-1/CXCL12 in the marrow (Fig S6), although the cellular source of this SDF-1/CXCL12 alteration is not clear as the frequency of osteoblast, a major source of SDF-1/CXCL12 [49, 50], is not obviously changed in mice receiving either ligand blocking antibody (Fig S8) (see below for further discussion on SDF-1/CXCL12). Because *RBP-J_K*-deficient mice respond with increased HSPC mobilization after receiving ligand-blocking antibodies, we conclude that the loss of Notch receptor-ligand engagement, or engagement-mediated non-canonical Notch effector functions, rather than the loss of *RBP-J_K*-dependent Notch transcriptional activation, is the major cause of HSPC exit from the marrow observed in *Mx1-Cre/Pofut1$^{F/F}$* mice and in the setting of Notch ligand antibody blockade.

Both Notch1 and Notch2 are expressed in mouse marrow HSPCs, with Notch2 being expressed at a much higher level than Notch1 [21, 51]. Notch2 is shown responsible for the enhanced generation of short-term and long-term repopulating stem cells during stress hematopoiesis [51]. We speculate that Notch2 is the major Notch receptor responsible for the HSPC adhesion to niche supporting cells, as a Notch2 cleavage-blocking antibody induces a more pronounced myeloid progenitor mobilization than the Notch1 cleavage-blocking antibody (data not shown). Interestingly, although deficiency of *Pofut1* is not associated with alteration of integrin expression on HSPCs, blocking Notch2 signaling modestly decreases HSPC expression of activated β1-integrin (data not shown). These observations suggest that the mechanism mediating HSPC egress in the case of loss of Notch adhesion is somewhat different form that mediating HSPC egress induced by the loss of Notch activation, which appears to affect integrin activation that is critical for the adhesion of HSPCs to the marrow microenvironment [52, 53]. Although decreased β1-integrin activation after blocking Notch signaling in marrow HSPC is consistent with findings in the vascular system where Notch activation promotes β1-integrin-mediated adhesion [54], the reason for the unaltered integrin activation in *Pofut1*-deficient HSPCs is unclear. The exact role of Notch2 and other Notch receptors in HSC niche retention is being investigated, and needs to be further verified in genetic mouse models.

Our previous studies showed that both cell-autonomous and stroma-dependent mechanisms contribute to the myeloproliferation observed in *Pofut1*-deficient mice [21]. Recent studies

suggested that G-CSF contributes to myeloproliferation non-cell-autonomously in mouse models of Notch down-regulation [55, 56]. Indeed, we found that plasma G-CSF amounts increase at 2-3 months after *Pofut1* deletion and contribute to excessive granulocytic differentiation (Wang et al., manuscript in preparation). However, plasma levels of G-CSF were not elevated at the earlier time when increased HSPC exit was identified in *Mx1-Cre/Pofut1*$^{F/F}$ mice. Nevertheless, other mechanism(s) may contribute to *Pofut1*-deficient HSPC proliferation and increased cycling. These may include *RBP-J*$_K$-independent Notch effectors inducing pathways that promote proliferation and increased cell cycling [57], or functional changes of adhesive molecules interacting with Notch or regulated by Notch [58, 59]. In addition, we cannot completely exclude the possibility that deletion of *Pofut1* results in Notch-unrelated effects, despite the highly similar phenotypes revealed by the *Pofut1*-deficient model and Notch ligand blocking antibodies. Moreover, increased egress of HSPCs is only observed in WT recipients receiving *Pofut1*-deficient marrow (Fig S1) and not *vice versa*. Since *Mx1* (+) stromal cells have osteolineage-restricted MSC features, it is possible *Mx1-Cre*-based deletion of *Pofut1* might affect *O*-fucose modification of Notch or Notch ligand in this cell population [60]. However, increased HSPC egress is not found in mice lacking *Pofut1* in osteoblastic progenitors (*Osterix-Cre/Pofut1*$^{F/F}$) (Wang et al, manuscript in preparation). In contrast to the significant osteolineage cell alterations in aged mice when Notch signaling is lost in osteoprogenitors [61], no significant changes in either osteoprogenitors or MSCs are observed in either *Pofut1*-deficient mice at the time of analysis, or in mice receiving blocking antibodies (Fig S8). Further, loss of *O*-fucose on Notch ligands has not been found to alter ligand expression or function [17, 62]. Therefore our combined data support a cell-autonomous mechanism underlying the enhanced egress of HSPCs due to the loss of *O*-fucosylglycans on Notch receptors.

Diverse factors coordinately regulate HSC stemness, proliferation and lineage commitment in the marrow microenvironment. SDF-1/CXCL12 expression by reticular and osteolineage cells supports HSC marrow retention and BBprogenitor development, whereas SDF-1 expressed by endothelial cells and peri-vascular mesenchymal progenitor cells supports HSC quiescence and HSC function [63, 64]. Surprisingly, we observe that, SDF-1/CXCL12 transcripts in marrow non-hematopoietic cells are elevated following *Pofut1* deletion, and they are also elevated after brief Notch ligand blockade, whereas the protein level of SDF-1 was not noticeably changed in *Pofut1*-deleted marrow but modestly decreased in the marrow plasma of mice receiving ligand blocking antibodies. Whether the observed HSC phenotypes from *Pofut1*-deficient mice are related to the alteration of specific SDF-1/CXCL12-expressing stromal elements, and whether Notch ligands cross-regulate SDF-1/CXCL12 in osteolineage cells or perivascular mesenchymal progenitor cells, remains unclear and warrants further investigation.

Finally, the observations from our studies suggest a therapeutic indication. Inadequate mobilization in HSPC transplantation remains a clinical problem. Our findings that either blocking Notch ligand or targeting Notch receptor-ligand binding increases HSPC emigration suggest a novel approach for enhancing HSPC mobilization for those patients responding poorly to current HSC mobilizing regimes.

Conclusions

In this study, we reveal that HSPC quiescence and retention in the marrow niche is facilitated by the interaction between Notch-expressing HSPCs and JAG1- or DLL4-expressing niche cells, dependent on the *O*-fucosylation of Notch. A loss of *O*-fucosyl modification of Notch, or disruption of Notch receptor-ligand binding by neutralizing antibodies, results in increased HSPC egress and HSPC mobilization.

Supplementary Material

Refer to Web version on PubMed Central for supplementary material.

Acknowledgments

We thank Dr. Guang Zhou for assisting in the isolation of calvarium osteoblasts. This work was supported by grants from American Cancer Society LIBB125064 (L.Z.), HL103827 (L.Z.), RO195022 (P.S.), RO1GM106417 (P. S.), MGH Federal Share of the Program Income under C06 CA059267, Proton Therapy Research and Treatment Center (V.W.C.Y.), BD Biosciences Stem Cell Grant (V.W.C.Y.), Bullock-Wellman Fellowship Award (V.W.C.Y.), Tosteson & Fund for Medical Discovery Fellowship (V.W.C.Y.), HL097794 (D.T.S.), HL044851 (D.T.S.), HL100402 (D.T.S), HL44851 (D.T.S.), HL96372 (D.T.S.) and EB14703 (D.T.S).

References

1. Wilson A, Trumpp A. Bone-marrow haematopoietic-stem-cell niches. Nat Rev Immunol. 2006; 6:93–106. [PubMed: 16491134]
2. Calvi LM, Adams GB, Weibrecht KW, et al. Osteoblastic cells regulate the haematopoietic stem cell niche. Nature. 2003; 425:841–846. [PubMed: 14574413]
3. Zhang J, Niu C, Ye L, et al. Identification of the haematopoietic stem cell niche and control of the niche size. Nature. 2003; 425:836–841. [PubMed: 14574412]
4. Kiel MJ, Yilmaz OH, Iwashita T, et al. SLAM family receptors distinguish hematopoietic stem and progenitor cells and reveal endothelial niches for stem cells. Cell. 2005; 121:1109–1121. [PubMed: 15989959]
5. Butler JM, Nolan DJ, Vertes EL, et al. Endothelial cells are essential for the self-renewal and repopulation of Notch-dependent hematopoietic stem cells. Cell Stem Cell. 2010; 6:251–264. [PubMed: 20207228]
6. Ding L, Saunders TL, Enikolopov G, Morrison SJ. Endothelial and perivascular cells maintain haematopoietic stem cells. Nature. 2012; 481:457–462. [PubMed: 22281595]
7. Sugiyama T, Kohara H, Noda M, Nagasawa T. Maintenance of the hematopoietic stem cell pool by CXCL12-CXCR4 chemokine signaling in bone marrow stromal cell niches. Immunity. 2006; 25:977–988. [PubMed: 17174120]
8. Sacchetti B, Funari A, Michienzi S, et al. Self-renewing osteoprogenitors in bone marrow sinusoids can organize a hematopoietic microenvironment. Cell. 2007; 131:324–336. [PubMed: 17956733]
9. Mendez-Ferrer S, Michurina TV, Ferraro F, et al. Mesenchymal and haematopoietic stem cells form a unique bone marrow niche. Nature. 2010; 466:829–834. [PubMed: 20703299]
10. Winkler IG, Barbier V, Wadley R, et al. Positioning of bone marrow hematopoietic and stromal cells relative to blood flow in vivo: serially reconstituting hematopoietic stem cells reside in distinct nonperfused niches. Blood. 2010; 116:375–385. [PubMed: 20393133]
11. Chow A, Lucas D, Hidalgo A, et al. Bone marrow CD169+ macrophages promote the retention of hematopoietic stem and progenitor cells in the mesenchymal stem cell niche. J Exp Med. 2011; 208:261–271. [PubMed: 21282381]
12. Fehon RG, Kooh PJ, Rebay I, et al. Molecular interactions between the protein products of the neurogenic loci Notch and Delta, two EGF-homologous genes in Drosophila. Cell. 1990; 61:523–534. [PubMed: 2185893]

13. Rebay I, Fleming RJ, Fehon RG, et al. Specific EGF repeats of Notch mediate interactions with Delta and Serrate: implications for Notch as a multifunctional receptor. Cell. 1991; 67:687–699. [PubMed: 1657403]
14. Wang Y, Shao L, Shi S, et al. Modification of epidermal growth factor-like repeats with O-fucose. Molecular cloning and expression of a novel GDP-fucose protein O-fucosyltransferase. J Biol Chem. 2001; 276:40338–40345. [PubMed: 11524432]
15. Luo Y, Haltiwanger RS. O-fucosylation of notch occurs in the endoplasmic reticulum. J Biol Chem. 2005; 280:11289–11294. [PubMed: 15653671]
16. Okajima T, Xu A, Lei L, Irvine KD. Chaperone activity of protein O-fucosyltransferase 1 promotes notch receptor folding. Science. 2005; 307:1599–1603. [PubMed: 15692013]
17. Okajima T, Irvine KD. Regulation of notch signaling by o-linked fucose. Cell. 2002; 111:893–904. [PubMed: 12526814]
18. Okajima T, Xu A, Irvine KD. Modulation of notch-ligand binding by protein O-fucosyltransferase 1 and fringe. J Biol Chem. 2003; 278:42340–42345. [PubMed: 12909620]
19. Shi S, Stanley P. Protein O-fucosyltransferase 1 is an essential component of Notch signaling pathways. Proc Natl Acad Sci U S A. 2003; 100:5234–5239. [PubMed: 12697902]
20. Okamura Y, Saga Y. Pofut1 is required for the proper localization of the Notch receptor during mouse development. Mech Dev. 2008; 125:663–673. [PubMed: 18547789]
21. Yao D, Huang Y, Huang X, et al. Protein O-fucosyltransferase 1 (Pofut1) regulates lymphoid and myeloid homeostasis through modulation of Notch receptor ligand interactions. Blood. 2011; 117:5652–5662. [PubMed: 21464368]
22. Zhou L, Li LW, Yan Q, et al. Notch-dependent control of myelopoiesis is regulated by fucosylation. Blood. 2008; 112:308–319. [PubMed: 18359890]
23. Cheng T, Rodrigues N, Shen H, et al. Hematopoietic stem cell quiescence maintained by p21cip1/waf1. Science. 2000; 287:1804–1808. [PubMed: 10710306]
24. Myers J, Huang Y, Wei L, et al. Fucose-deficient hematopoietic stem cells have decreased self-renewal and aberrant marrow niche occupancy. Transfusion. 2010; 50:2660–2669. [PubMed: 20573072]
25. Ridgway J, Zhang G, Wu Y, et al. Inhibition of Dll4 signalling inhibits tumour growth by deregulating angiogenesis. Nature. 2006; 444:1083–1087. [PubMed: 17183323]
26. Broxmeyer HE, Orschell CM, Clapp DW, et al. Rapid mobilization of murine and human hematopoietic stem and progenitor cells with AMD3100, a CXCR4 antagonist. J Exp Med. 2005; 201:1307–1318. [PubMed: 15837815]
27. Zhou G, Zheng Q, Engin F, et al. Dominance of SOX9 function over RUNX2 during skeletogenesis. Proc Natl Acad Sci U S A. 2006; 103:19004–19009. [PubMed: 17142326]
28. Christensen JL, Wright DE, Wagers AJ, Weissman IL. Circulation and chemotaxis of fetal hematopoietic stem cells. PLoS Biol. 2004; 2:E75. [PubMed: 15024423]
29. Shim, J. Department of Pathology. University of Michigan; Ann Arbor: 2009. Biophysical determinants of Notch signaling.; p. 168
30. Myers JT, Barkauskas DS, Huang AY. Dynamic Imaging of Marrow-Resident Granulocytes Interacting with Human Mesenchymal Stem Cells upon Systemic Lipopolysaccharide Challenge. Stem Cells Int. 2013; 2013:656839. [PubMed: 23606861]
31. Zhang J, Grindley JC, Yin T, et al. PTEN maintains haematopoietic stem cells and acts in lineage choice and leukaemia prevention. Nature. 2006; 441:518–522. [PubMed: 16633340]
32. Min IM, Pietramaggiori G, Kim FS, et al. The transcription factor EGR1 controls both the proliferation and localization of hematopoietic stem cells. Cell Stem Cell. 2008; 2:380–391. [PubMed: 18397757]
33. Ge C, Liu T, Hou X, Stanley P. In vivo consequences of deleting EGF repeats 8-12 including the ligand binding domain of mouse Notch1. BMC Dev Biol. 2008; 8:48. [PubMed: 18445292]
34. Ge C, Stanley P. The O-fucose glycan in the ligand-binding domain of Notch1 regulates embryogenesis and T cell development. Proc Natl Acad Sci U S A. 2008; 105:1539–1544. [PubMed: 18227520]

35. Simmons PJ, Levesque JP, Zannettino AC. Adhesion molecules in haemopoiesis. Baillieres Clin Haematol. 1997; 10:485–505. [PubMed: 9421612]
36. Kunisaki Y, Bruns I, Scheiermann C, et al. Arteriolar niches maintain haematopoietic stem cell quiescence. Nature. 2013; 502:637–643. [PubMed: 24107994]
37. Karanu FN, Murdoch B, Gallacher L, et al. The notch ligand jagged-1 represents a novel growth factor of human hematopoietic stem cells. J Exp Med. 2000; 192:1365–1372. [PubMed: 11067884]
38. Weber JM, Forsythe SR, Christianson CA, et al. Parathyroid hormone stimulates expression of the Notch ligand Jagged1 in osteoblastic cells. Bone. 2006; 39:485–493. [PubMed: 16647886]
39. Yan M, Callahan CA, Beyer JC, et al. Chronic DLL4 blockade induces vascular neoplasms. Nature. 2010; 463:E6–7. [PubMed: 20147986]
40. Kopp HG, Hooper AT, Avecilla ST, Rafii S. Functional heterogeneity of the bone marrow vascular niche. Ann N Y Acad Sci. 2009; 1176:47–54. [PubMed: 19796232]
41. Purton LE, Bernstein ID, Collins SJ. All-trans retinoic acid enhances the long-term repopulating activity of cultured hematopoietic stem cells. Blood. 2000; 95:470–477. [PubMed: 10627451]
42. Arai F, Hirao A, Ohmura M, et al. Tie2/angiopoietin-1 signaling regulates hematopoietic stem cell quiescence in the bone marrow niche. Cell. 2004; 118:149–161. [PubMed: 15260986]
43. Adams GB, Chabner KT, Alley IR, et al. Stem cell engraftment at the endosteal niche is specified by the calcium-sensing receptor. Nature. 2006; 439:599–603. [PubMed: 16382241]
44. Yang L, Wang L, Geiger H, et al. Rho GTPase Cdc42 coordinates hematopoietic stem cell quiescence and niche interaction in the bone marrow. Proc Natl Acad Sci U S A. 2007; 104:5091–5096. [PubMed: 17360364]
45. Murata A, Okuyama K, Sakano S, et al. A Notch ligand, Delta-like 1 functions as an adhesion molecule for mast cells. J Immunol. 2010; 185:3905–3912. [PubMed: 20810995]
46. Murata A, Yoshino M, Hikosaka M, et al. An evolutionary-conserved function of Mammalian notch family members as cell adhesion molecules. PLoS One. 2014; 9:e108535. [PubMed: 25255288]
47. Guezguez B, Campbell CJ, Boyd AL, et al. Regional localization within the bone marrow influences the functional capacity of human HSCs. Cell Stem Cell. 2013; 13:175–189. [PubMed: 23910084]
48. Noguera-Troise I, Daly C, Papadopoulos NJ, et al. Blockade of Dll4 inhibits tumour growth by promoting non-productive angiogenesis. Nature. 2006; 444:1032–1037. [PubMed: 17183313]
49. Semerad CL, Christopher MJ, Liu F, et al. G-CSF potently inhibits osteoblast activity and CXCL12 mRNA expression in the bone marrow. Blood. 2005; 106:3020–3027. [PubMed: 16037394]
50. Christopher MJ, Liu F, Hilton MJ, et al. Suppression of CXCL12 production by bone marrow osteoblasts is a common and critical pathway for cytokine-induced mobilization. Blood. 2009; 114:1331–1339. [PubMed: 19141863]
51. Varnum-Finney B, Halasz LM, Sun M, et al. Notch2 governs the rate of generation of mouse long- and short-term repopulating stem cells. J Clin Invest. 2011
52. Taniguchi Ishikawa E, Chang KH, Nayak R, et al. Klf5 controls bone marrow homing of stem cells and progenitors through Rab5-mediated beta1/beta2-integrin trafficking. Nat Commun. 2013; 4:1660. [PubMed: 23552075]
53. Papayannopoulou T, Priestley GV, Nakamoto B, et al. Synergistic mobilization of hemopoietic progenitor cells using concurrent beta1 and beta2 integrin blockade or beta2-deficient mice. Blood. 2001; 97:1282–1288. [PubMed: 11222371]
54. Leong KG, Hu X, Li L, et al. Activated Notch4 inhibits angiogenesis: role of beta 1-integrin activation. Mol Cell Biol. 2002; 22:2830–2841. [PubMed: 11909975]
55. Yoda M, Kimura T, Tohmonda T, et al. Dual functions of cell-autonomous and non-cell-autonomous ADAM10 activity in granulopoiesis. Blood. 2011; 118:6939–6942. [PubMed: 22042698]
56. Wang L, Zhang H, Rodriguez S, et al. Notch-dependent repression of miR-155 in the bone marrow niche regulates hematopoiesis in an NF-kappaB-dependent manner. Cell Stem Cell. 2014; 15:51–65. [PubMed: 24996169]

57. Huber RM, Rajski M, Sivasankaran B, et al. Deltex-1 activates mitotic signaling and proliferation and increases the clonogenic and invasive potential of U373 and LN18 glioblastoma cells and correlates with patient survival. PLoS One. 2013; 8:e57793. [PubMed: 23451269]
58. Kishi N, Tang Z, Maeda Y, et al. Murine homologs of deltex define a novel gene family involved in vertebrate Notch signaling and neurogenesis. Int J Dev Neurosci. 2001; 19:21–35. [PubMed: 11226752]
59. Hu QD, Ang BT, Karsak M, et al. F3/contactin acts as a functional ligand for Notch during oligodendrocyte maturation. Cell. 2003; 115:163–175. [PubMed: 14567914]
60. Park D, Spencer JA, Koh BI, et al. Endogenous bone marrow MSCs are dynamic, fate-restricted participants in bone maintenance and regeneration. Cell Stem Cell. 2012; 10:259–272. [PubMed: 22385654]
61. Hilton MJ, Tu X, Wu X, et al. Notch signaling maintains bone marrow mesenchymal progenitors by suppressing osteoblast differentiation. Nat Med. 2008; 14:306–314. [PubMed: 18297083]
62. Muller J, Rana NA, Serth K, et al. O-fucosylation of the notch ligand mDLL1 by POFUT1 is dispensable for ligand function. PLoS One. 2014; 9:e88571. [PubMed: 24533113]
63. Greenbaum A, Hsu YM, Day RB, et al. CXCL12 in early mesenchymal progenitors is required for haematopoietic stem-cell maintenance. Nature. 2013; 495:227–230. [PubMed: 23434756]
64. Ding L, Morrison SJ. Haematopoietic stem cells and early lymphoid progenitors occupy distinct bone marrow niches. Nature. 2013; 495:231–235. [PubMed: 23434755]

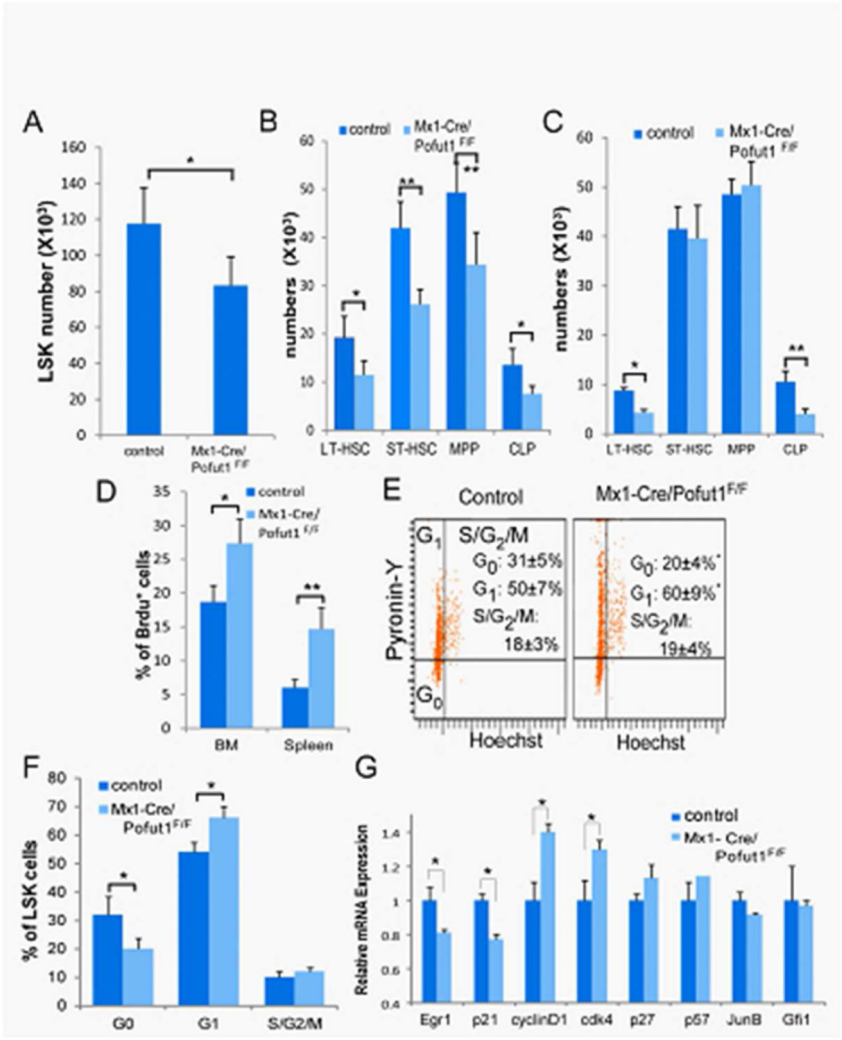

Figure 1. *Pofut1* deficiency leads to transient HSPC reduction in the marrow and HSPC proliferation

Mice of 5-6 weeks were injected with pIpC to induce *Pofut1* deletion in *Mx1-Cre/Pofut1* $^{F/F}$ mice. The frequencies of total marrow LSK ($Lin^-Sca\text{-}1^+c\text{-}kit^+$) (A), CLP ($Lin^-IL7R^+Sca\text{-}1^+c\text{-}kit^+$) and HSC subpopulations, including LT-HSC ($Flt3^-CD34^-LSK$), S-HSC ($Flt3^-CD34^+LSK$) and MPP ($Flt3^+CD34^+LSK$) (B), were determined from 2 femurs and 2 tibias from *Mx1-Cre/Pofut1* $^{F/F}$ mice (n=7) or control mice (*Pofut1*$^{F/F}$ or *Mx1-Cre/Pofut1* $^{F/+}$) (n=5) 4 weeks after pIpC injection. (C) The frequencies of CLP and HSC subpopulations were determined 4-5 months after *Pofut1* deletion in control (n=5) or *Mx1-Cre/Pofut1*$^{F/F}$ (n=6) mice. (D) BrdU incorporation of *Mx1-Cre/Pofut1*$^{F/F}$ mice or control mice myeloid progenitor cells was determined by FACS (n=5). (E) Marrow cells were stained with FITC-labeled lineage antibodies (CD4, CD8, B220, Gr-1, CD11b, TER119, and NK1.1), APC-anti-c-kit, PE-anti-Sca-1, pyronin Y (RNA dye), and Hoechst 33342 (DNA dye). The relative proportion of cells in G_0, G_1 and S-G_2/M phase of the cell cycle was analyzed on gated LSK cells. Results are presented as averages ± SD (n=4). (F) Three months after transplantation of 2 × 10^6 marrow cells from *Mx1-Cre/Pofut1*$^{F/F}$ mice or control mice into lethally-irradiated WT recipient mice, marrow cells in the G_0, G_1 and S-

G_2/M phase of the cell cycle were analyzed as described in (E) (n=4 in each group). (G) Relative mRNA transcript levels of *cyclin D1, p21, EGR1, p27, p53, JunB, and Gfi11* in LT-HSC cells were measured by real-time quantitative RT-PCR and normalized to the WT LT-HSC GAPDH mRNA transcripts (n=6). Mice 2-3 months old were used in experiments of D-G for direct analysis or as donors. Results in A-G are presented as averages ± SD. Student *t* test was performed. * $p<0.05$, ** $p<0.01$

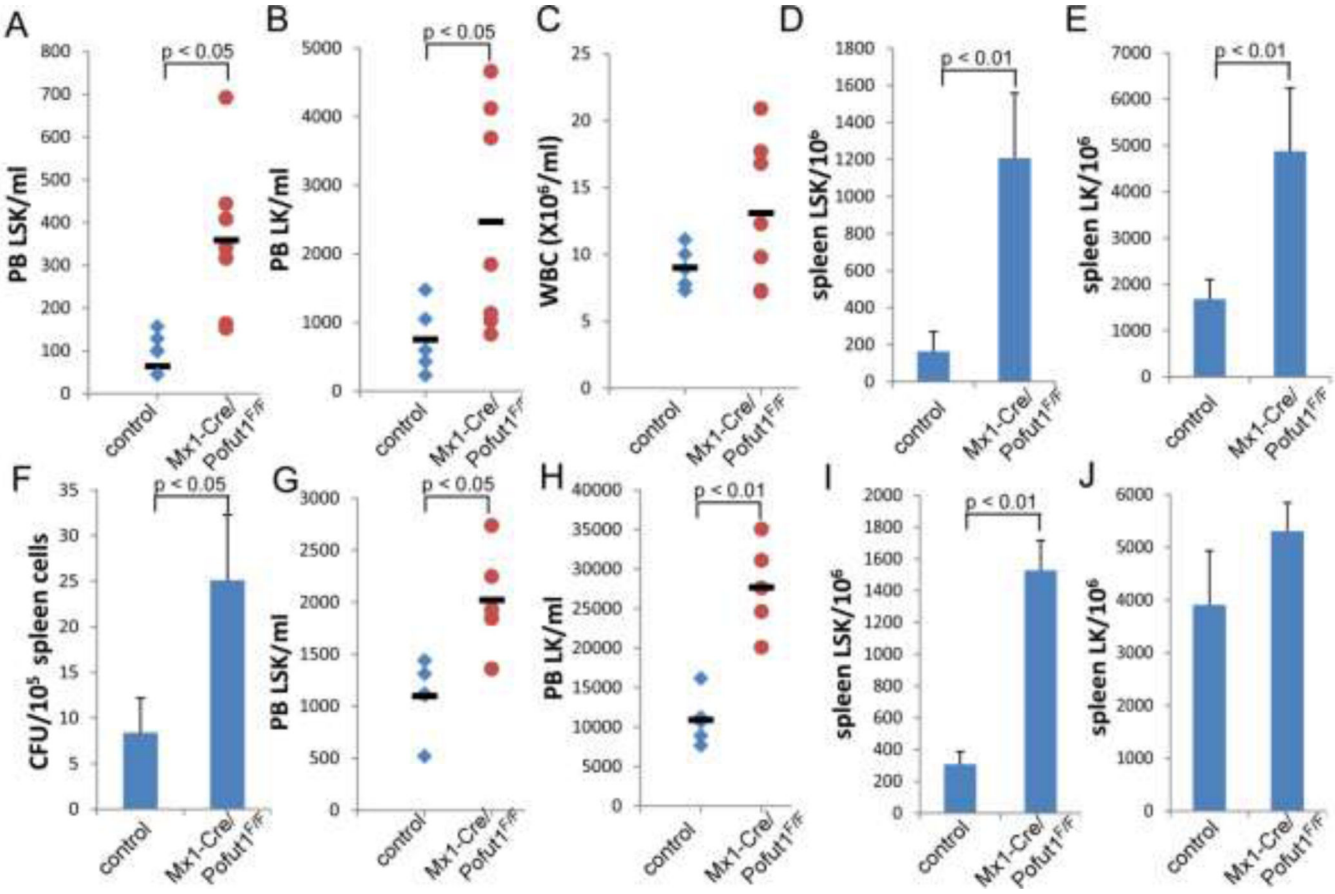

Figure 2. *Pofut1* deficiency leads to enhanced HSPC exit from the marrow and mobilization

Three to four weeks after pIpC injection, HSPCs present in the periphery and in spleen were determined by FACS analysis. Shown are total numbers of LSK cells (A), LK cells (B) and white blood cell counts (C) per ml of blood from *Mx1-Cre/Pofut1*$^{F/F}$ mice (n=7) and control mice (n=5). (D-F) Shown are the frequencies of LSK (D) and LK (E) cells per million nucleated cells, and the total number of colony forming units (CFU) (F) in the spleen of *Mx1-Cre/Pofut1*$^{F/F}$ and control mice. (G-J) Circulating and spleen-residing HSPC frequencies were determined after mobilization. Mobilization was induced by 2.5 μg G-CSF or PBS twice daily for 2 days, followed by subcutaneous injection of 5 mg/kg AMD3100. One hour later, the mobilized LSK (G) or LK (H) cells in peripheral blood (PB) and in spleen (I-J) were determined by FACS analysis. Results are presented as mean ± SD (n=5-7 for each group of mice). Student *t* test was performed; *p* values were >0.05 unless shown in the figure.

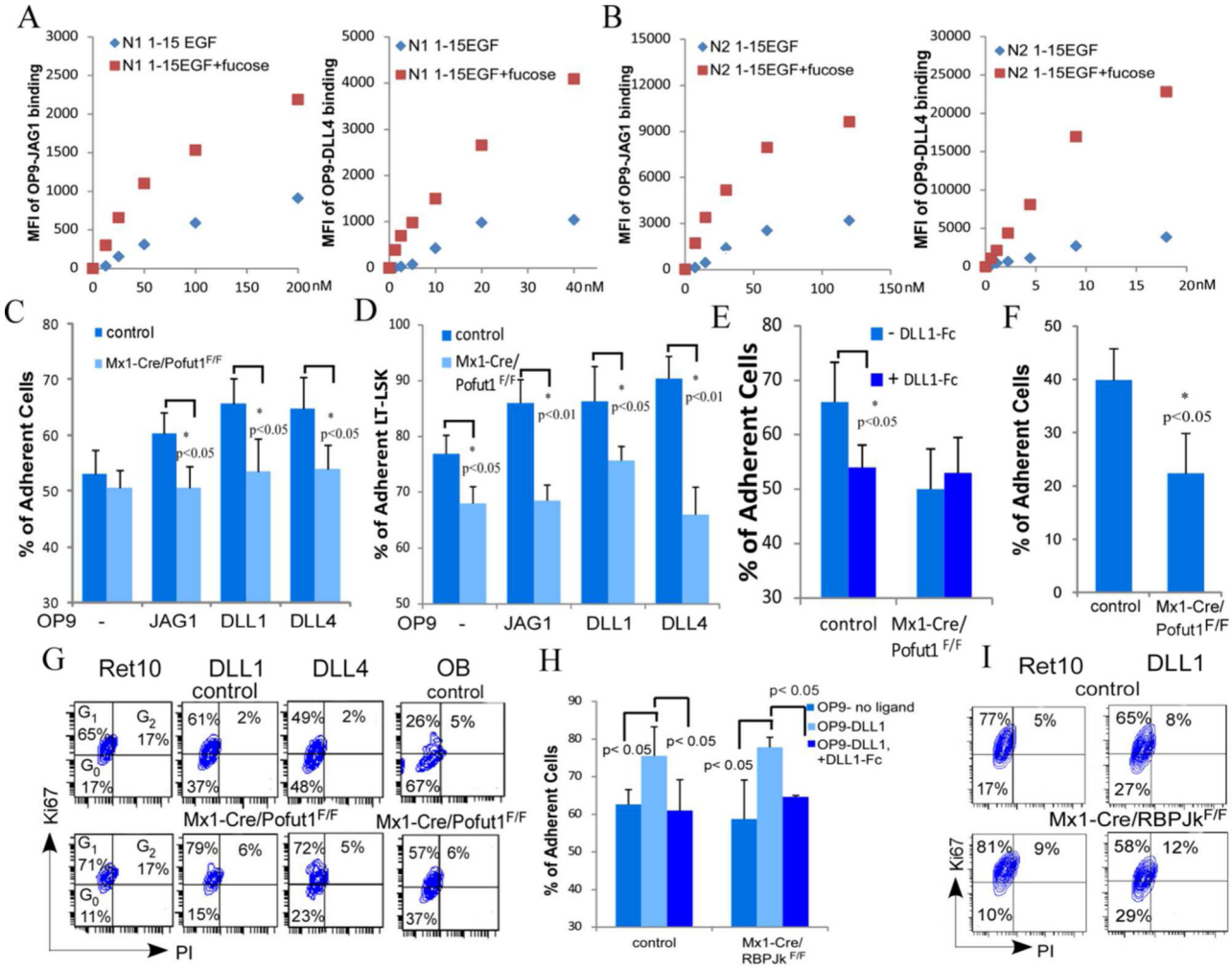

Figure 3. Decreased adhesion and increased cell cycling of *Pofut1*-deficient HSPCs

(A-B) Recombinant soluble Notch1 and Notch2 ECD fragments comprising 1-15 EGF-like repeats fused to human IgG Fc were made from FX-deficient CHO cells in the presence (N1 1-15EGF+fucose & N2 1-15EGF+fucose; squares) or absence (N1 1-15EGF & N2 1-15EGF; diamonds) of fucose. Binding of N1 (A) and N2 (B) chimerics to OP9-JAG1 or OP9-DLL4 cells was analysed by FACS using PE-anti-human IgG. (C) 1.5×10^5 LK cells were co-cultured with confluent OP9 cells bearing Notch ligands. Non-adherent cells were counted and compared with those from co-cultures with control OP9 cells bearing no Notch ligand. (D) The frequencies of non-adherent $CD48^-$ $CD150^+$LSK cells were quantified by FACS and the proportion of adherent cells was calculated by subtracting non-adherent cells from input cells. (E) 2.0×10^5 LK cells were pre-incubated with recombinant DLL1-Fc (D1-Fc, 30 μg/ml) and then co-cultured with OP9-DLL1 cells in the presence of D1-Fc. Non-adherent cells were counted and compared with those from co-cultures lacking D1-Fc. (F) Confluent calvarium GFP^+ cells from col2.3-GFP mice were co-cultured with 2.0×10^5 LK cells from control or *Mx1-Cre/Pofut1*$^{F/F}$ mice, respectively. Non-adherent cells were enumerated and compared. (G) After co-culture of 5×10^3 LSK cells with OP9-control (Ret10), OP9-DLL1 or OP9-DLL4 for 48 hrs in the presence of cytokine cocktail (25 ng/ml

SCF, 10 ng/ml Flt3 ligand and 5 ng/ml IL7), Sca-1^{+}Lin^{-} cells were gated and analyzed for cell cycling. (H) LK cells isolated from *Mx1-Cre/RBP-*$J_k^{F/F}$ or controls (*Mx1*-Cre/*RBP-*$Jk^{F/+}$) were co-cultured with confluent OP9-DLL1 and the adherent assay was performed. Another group of LKs were pre-incubated with recombinant D1-Fc (30 μg/ml) and then co-cultured with OP9 cells in the presence of D1-Fc. Non-adherent cells were counted and compared with those from co-cultures in the absence of D1-Fc. (I) After co-culture of LSKs with Ret10 or OP9-DLL1 for 48 hrs, Sca-1^{+}Lin^{-} cells were gated and analyzed for cell cycling. Data shown in A-B, G and I were representatives of 4 similar experiments. Data shown in C-F and H are presented as averages ±SD of 6 biological replicas. Student *t* test was performed; *p* values were >0.05 unless shown in the figure.

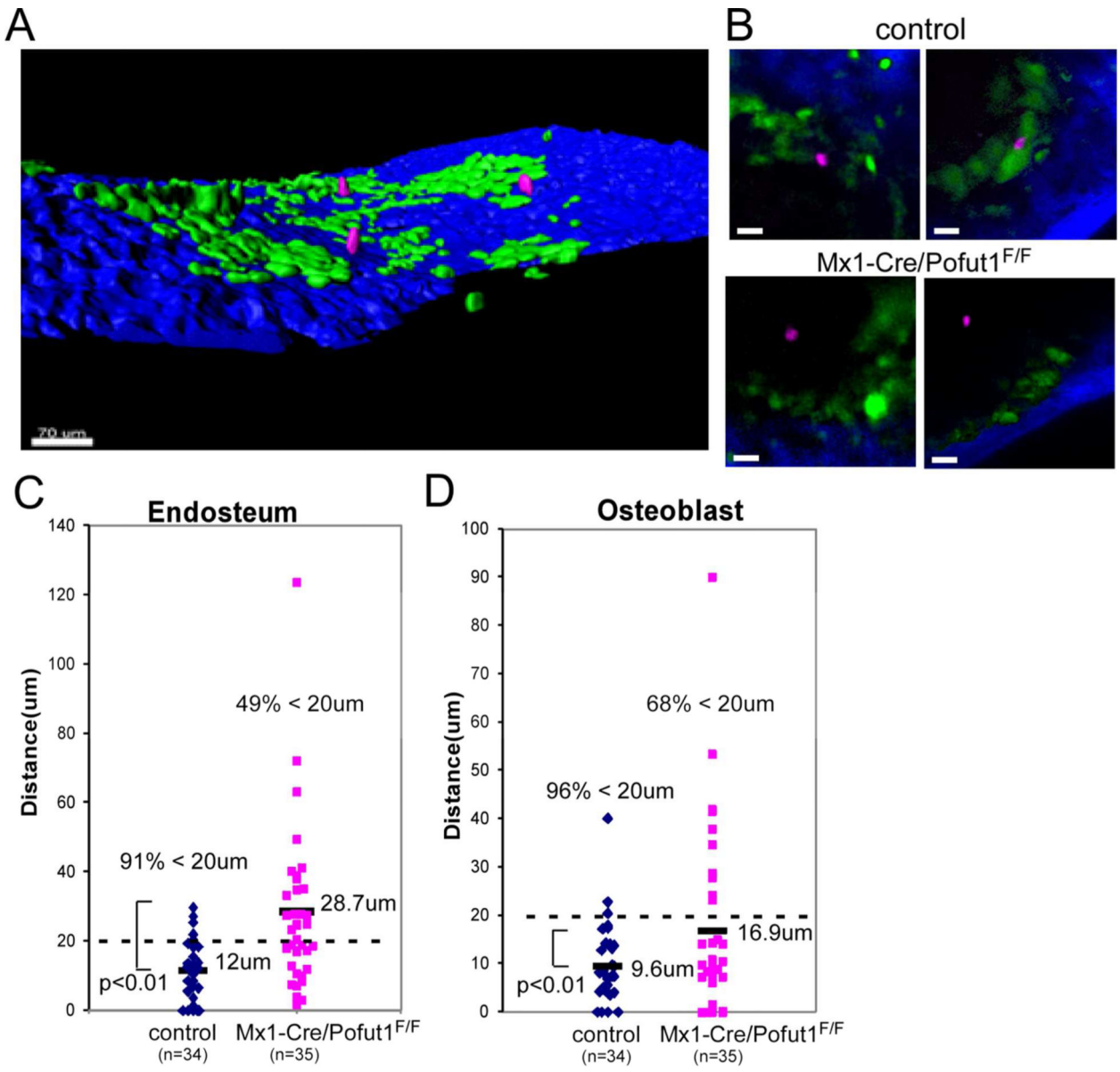

Figure 4. *Pofut1*-deficient LSK cells are localized more distal to the endosteum and osteoblasts

(A) A 3D image of femur marrow showing a close association between transplanted LSKs with osteoblasts and the endosteum in col2.3-GFP mice. LSK cells were labeled with SNARF. The endosteum is highlighted by the blue second harmonic signal, and osteoblastic cells are GFP-positive. The size bar is 70 μm. (B) Representative 2D images show the locations of control or *Pofut1*-deficient LSK cells relative to the endosteum and osteoblastic cells in femurs 24 hrs after being injected into irradiated col2.3-GFP mice. The size bar is 20 μm. (C-D) The shortest 3D distances between the LSK cells and the endosteum, represented by the blue signal (C), and GFP-positive osteoblastic cells (D), were compared for control and *Pofut1*-deficient cells. Data shown in C-D were pooled from 5 mice in each group. Student *t* test was performed.

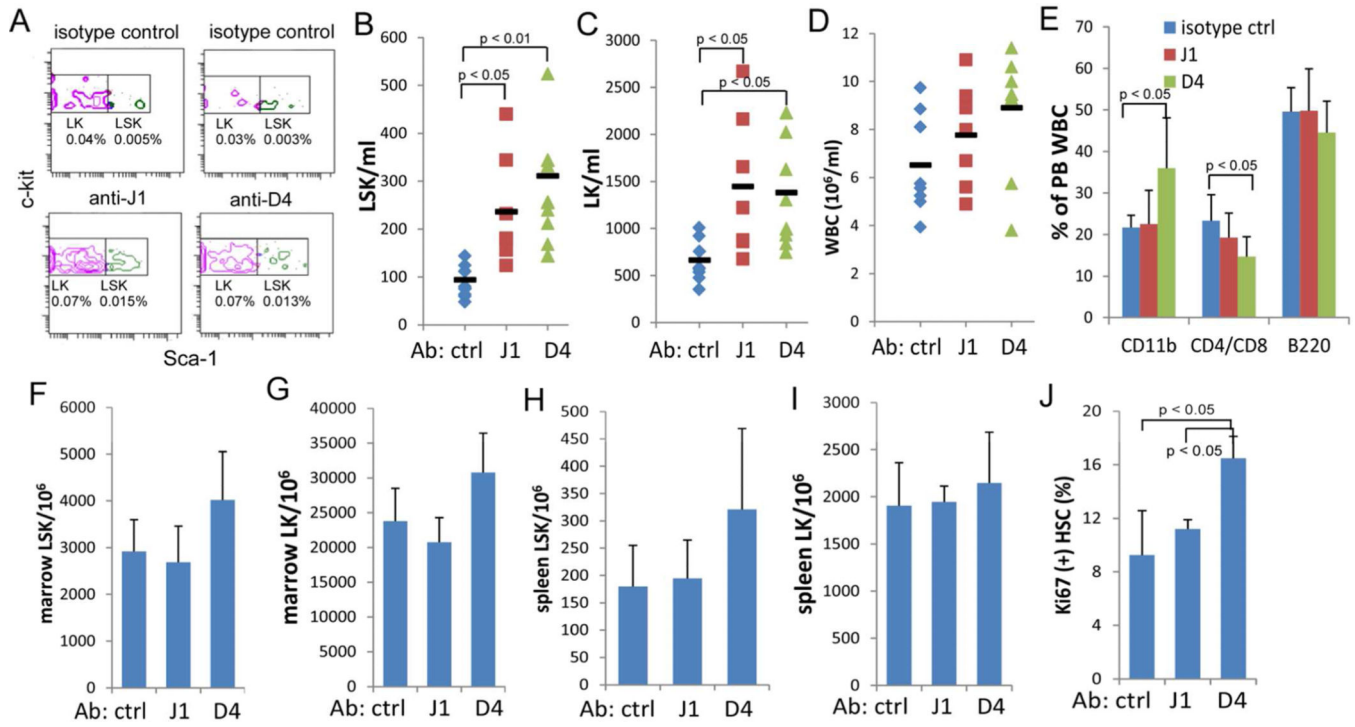

Figure 5. Antagonizing DLL4 or JAG1 binding to Notch promotes HSPC exit from the marrow

Mice received either 4 doses of isotype control (n=8; diamonds), anti-JAG1 (J1) (n=7; squares), or anti-DLL4 (D4) (n=8; triangles) antibodies, at 15 mg/kg body weight, 3-4 days apart, for 2 weeks. Four days after applying the last dose of antibody, PB, marrow and spleen were collected and analyzed for the frequencies of HSPC (LSK and LK). (A) Shown are representative FACS profiles displaying percentages of LSK and LK cells in PB mononuclear cells after red cell lysis followed by FACS analysis after gating on $Lin^{-}cBkit^{+}$ cells. (BBD) Shown are total numbers of LSK cells (B), LK cells (C), and white blood cells (D) in the PB of mice receiving blocking antibodies or isotype control antibodies. (E) The frequencies of granulocytes (CD11b+), T lymphocytes (CD4/CD8+), and B lymphocytes (-220+) present in each group of mice. The frequencies of LSK and LK cells per million total nucleated cells present in marrow (F-G) and in spleen (H-I) in each group of mice. (J) Proliferating LSK cells in the marrow were determined by Ki67 labeling. Results are presented as averages ± SD (n=7-8 in each group). Student *t* test was performed; *p* values were >0.05 unless shown in the figure.

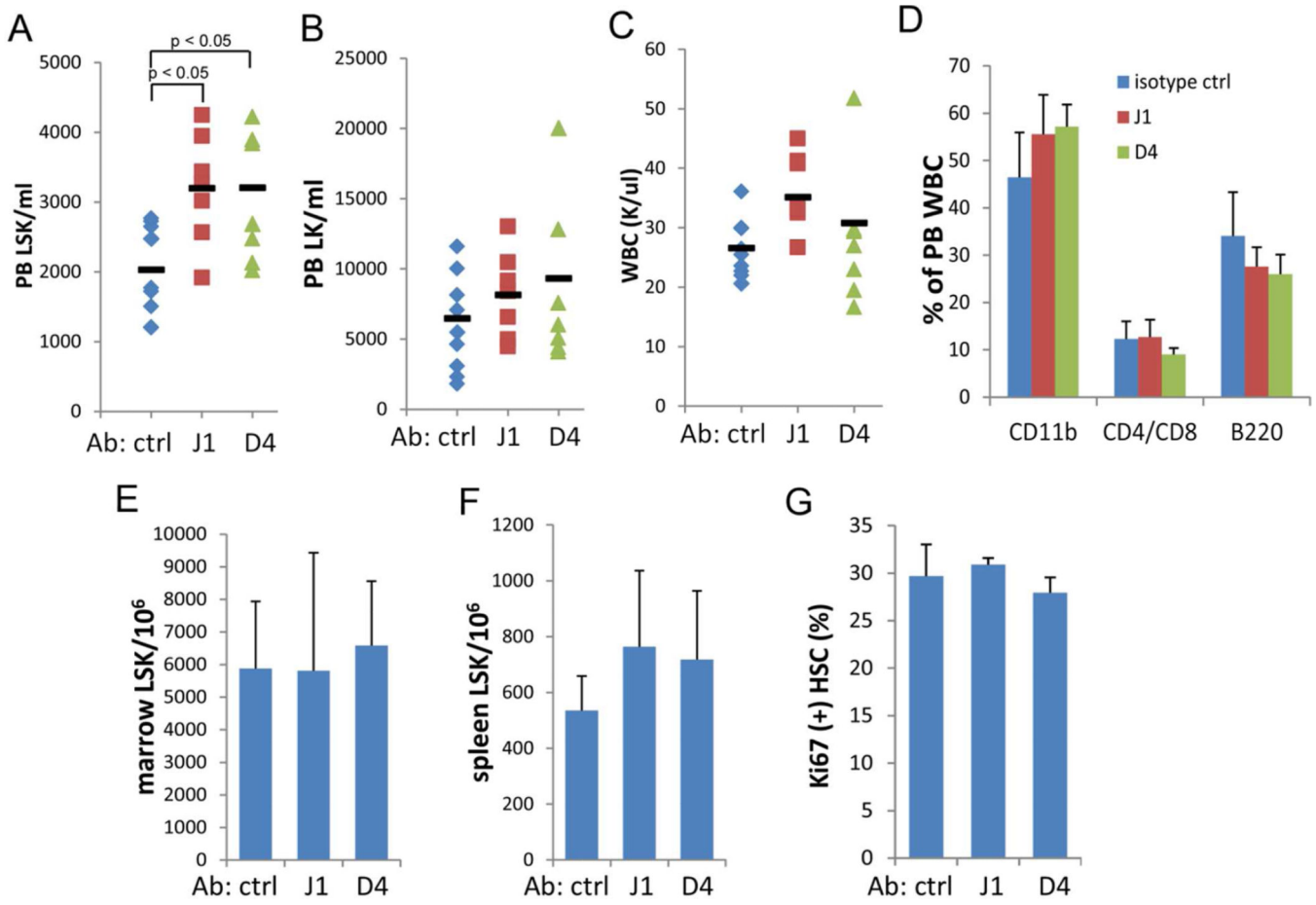

Figure 6. Antagonizing DLL4- or JAG1-Notch interactions further enhances HSPC mobilization

(A-B) Three to four days after the last dose of antibody treatment (isotype control, diamonds; anti-J1, squares; anti-D4, triangles), mice received the mobilizing regimen as described in Fig 2. The mobilized LSK (A) or LK cells (B) in PB were determined by FACS analysis. (C-D) Total white blood cells and the percentage of granulocytes, T and B cells were determined as in Fig 6D-E. Frequencies of LSK cells in the marrow (E) and in spleen (F) were determined by FACS. Proliferating LSK cells in the marrow were determined by Ki67 labeling (G). Results are presented as averages ± SD (n=7-9 in each group). Student *t* test was performed; *p* values were >0.05 unless shown in the figure.

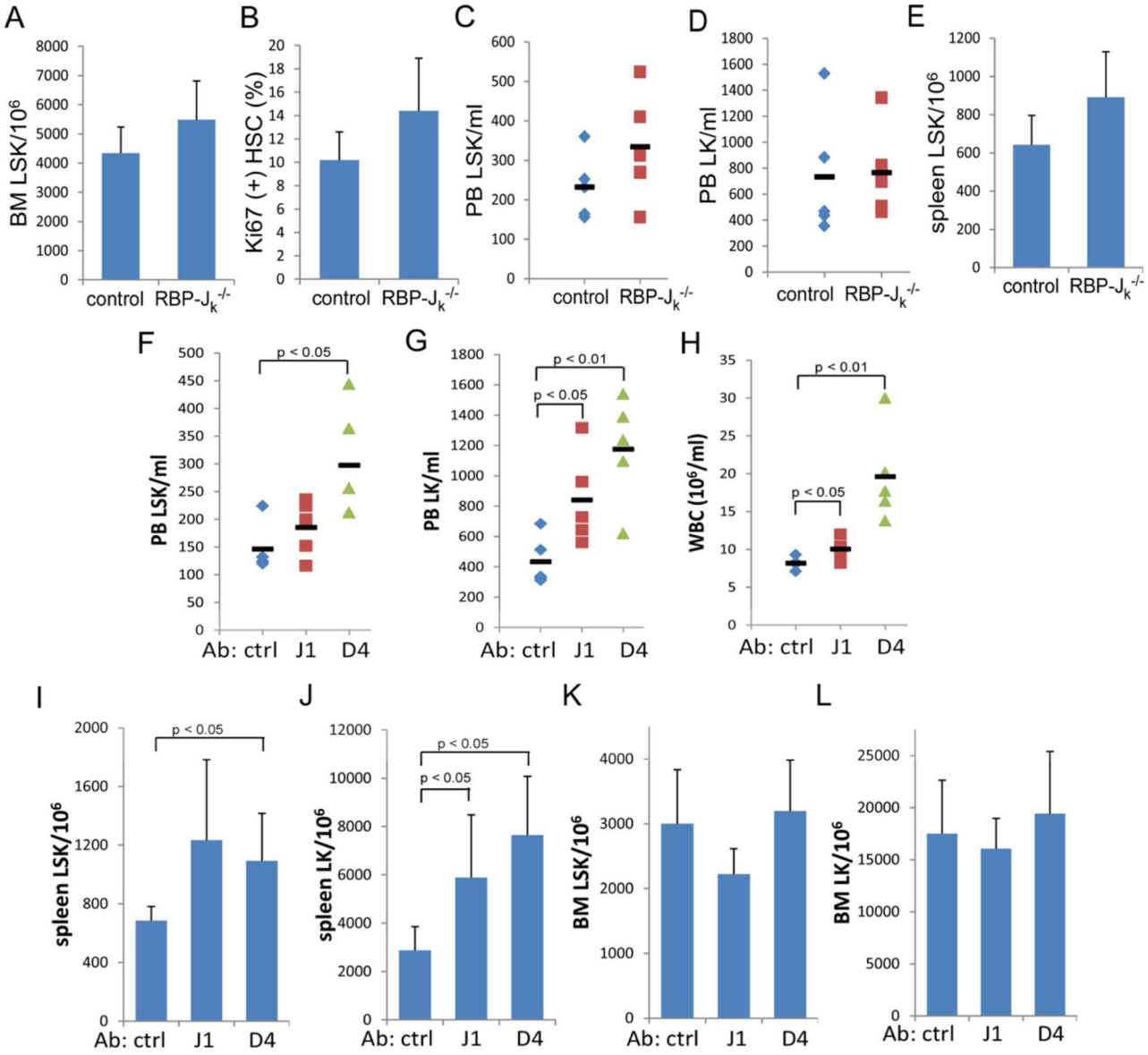

Figure 7. *Mx1-Cre/RBP-J$_k^{F/F}$* mice have mildly increased HSPC egress in the steady state but still display significant increases in HSPC egress responding to DLL4 or JAG1 ligand blockade

Following pIpC injection, the frequencies of LSK (A) and LK cells (not shown) in the bone marrow of *Mx1-Cre/RBP-J$_k^{F/F}$* (RBP-J$_k^{-/-}$) mice and control mice were determined by FACS analysis. (B) The proliferating LSK cells in the marrow were determined by Ki67 labeling. (C-E) The frequencies of LSK and LK cells in the peripheral blood and the frequency of spleen-residing LSK cells in *Mx1-Cre/RBP-J$_k^{F/F}$* (RBP-J$_k^{-/-}$) mice were determined by FACS. For ligand neutralizing experiment, *Mx1-Cre/RBP-J$_k^{F/F}$* mice received either 4 doses of isotype control (n=5), anti-JAG1 (J1) (n=5), or anti-DLL4 (D4) (n=5) antibodies, at 15 mg/kg body weight, 3-4 days apart, for 2 weeks. Four days after injecting the last dose of the antibody, PB, marrow and spleens were collected and analyzed for the frequencies of LSK and LK cells. The frequencies of LSK and LK cells in the peripheral blood (F-G), peripheral blood white cell counts (H), the frequencies of spleen-

residing (I-J) and bone marrow LSK and LK cells and (K-L) in *Mx1-Cre/RBP-*$J_k^{F/F}$ (*RBP-*$J_k^{-/-}$) mice were determined by FACS. Results are presented as averages ± SD. Student *t* test was performed; *p* values were >0.05 unless shown in the figure.